The Chemical Nature of Hydrogen Bonding in Proteins via NMR: *J*-Couplings, Chemical Shifts, and AIM Theory

William D. Arnold and Eric Oldfield*

Contribution from the Department of Chemistry, University of Illinois at Urbana-Champaign, 600 South Mathews Avenue, Urbana, Illinois 61801

Received July 13, 2000. Revised Manuscript Received October 2, 2000

Abstract: The trans hydrogen bond $^{3h}J_{NC'}$ coupling observed between peptide groups in proteins is shown to be mediated by a closed shell, noncovalent interaction between the donor hydrogen atom and the acceptor oxygen atom. The magnitude of $^{3h}J_{NC'}$ is shown to be an exponential function of the mutual penetration of the nonbonding van der Waals shells of the isolated donor and acceptor fragments. Our results also show that the magnitude of J_{FF}, the through-space coupling between two nonbonded fluorine nuclei in organic molecules and in a protein, exhibits a similar exponential dependence upon penetration of nonbonding monomer charge densities. These results support the idea that the existence of electron-coupled nuclear spin−spin coupling requires neither a covalent bond nor an attractive electrostatic bond between the coupled nuclei. By relating the results of calculations using Bader's theory of Atoms in Molecules, (Bader, R. F. W. *Atoms in Molecules−A Quantum Theory*; Clarendon Press: Oxford, 1990) to these couplings and to ^{1}H chemical shifts in proteins and model systems, a simple chemical description of protein backbone hydrogen bonds, the short, strong hydrogen bonds implicated in enzyme catalysis, as well as low-barrier hydrogen bonds, is obtained. Unlike protein backbone hydrogen bonds, the short, strong hydrogen bonds in enzymes have partial covalent character, which is shown to increase exponentially as the ^{1}H nucleus becomes more deshielded. Between ca. 20 and 21 ppm, the chemical shift region of experimentally observed low-barrier hydrogen bonds, the hydrogen bond becomes a fully covalent, shared-electron interaction.

Introduction

The recent observation of scalar couplings between nuclear spins spanned by a hydrogen bond in proteins has invigorated the discussion about the chemical nature of biological hydrogen bonds.[1−7] While the existence of these trans hydrogen bond couplings has led some to conclude that the bonds must be partially covalent,[4,8,9] nothing in the physical basis of scalar coupling requires this to be the case.[10,11] For example, the existence of noncovalent, long-range, through-space *J*-couplings in simple organic molecules has been known for over 40 years,[12] and over 20 years ago, Kimber et al.[13] demonstrated the occurrence of *J*-couplings between amino acid side chains separated by some 127 residues in the protein dihydrofolate reductase. Elucidating what may be legitimately implied about the character of a hydrogen bond from its NMR observables is likely to be of some importance in furthering our understanding about both protein (and nucleic acid) structure and function. For some time we have made an effort to establish structural−spectroscopic correlations in proteins, particularly between local geometry and the chemical shielding of $^{13}C^{\alpha}$ and $^{13}C^{\beta}$ atoms.[14−17] In the current situation, it appears that hydrogen bond *J*-couplings and chemical shifts may provide interesting new information about the nature of biological hydrogen bonds, particularly the low-barrier hydrogen bonds (LBHB) which are postulated as transition states in several enzyme catalytic events,[18−25] and are thought to have significant covalent character.[20,25−27] To help

(1) Cornilescu, G.: Ramirez, B. E.; Frank, M. K.; Clore, G. M.; Gronenborn, A. M.; Bax, A. *J. Am. Chem. Soc.* **1999**, *121*, 6275−6279.
(2) Wang, Y.-X.; Jacob, J.; Cordier, F.; Wingfield, P.; Stahl, S. J.; Lee-Huang, S.; Torchia, D.; Grzesiek, S.; Bax, A. *J. Biomol. NMR* **1999**, 14, 181−184.
(3) Cordier, F.; Grzesiek, S. *J. Am. Chem. Soc.* **1999**, *121*, 1601−1602.
(4) Cornilescu, G.; Hu, J.-S.; Bax, A. *J. Am. Chem. Soc.* **1999**, *121*, 2949−2950.
(5) Cordier, F.; Rogowski, M.; Grzesiek. S.; Bax, A. *J. Magn. Reson.* **1999**, *140*, 510−512.
(6) Meissner, A.; Sorensen, O. W. *J. Magn. Reson.* **2000**, *143*, 431−434.
(7) Scheurer, C.; Brüschweiler, R. *J. Am. Chem. Soc.* **1999**, *121*, 8661−8662.
(8) van der Vaart, A.; Merz, K. M., Jr. *J. Am. Chem. Soc.* **1999**, *121*, 9182−9190.
(9) Benedict, H.; Shenderovich, I. G.; Malkina, O. L.; Malkin, V. G.; Denisov, G. S.; Golubev, N. S.; Limbach, H.-H. *J. Am. Chem. Soc.* **2000**, *122*, 1979−1988.
(10) Dixon, W. T. *Theory and Interpretation of Magnetic Resonance Spectra*; Plenum Press: London, 1972.
(11) Bovey, F. A.; Jelinski, L.; Mirau, P. A. *Nuclear Magnetic Resonance Spectroscopy*, 2nd ed.; Academic Press: San Diego, 1988.
(12) Petrakis, L.; Sederholm, C. H. *J. Chem. Phys.* **1961**, *35*, 1243−1248.
(13) Kimber, B. J.; Feeney, J.; Roberts, G. C. K.; Birdsall, B.; Griffiths, D. V.; Burgen, A. S. V.; Sykes, B. D. *Nature* **1978**, *271*, 184−185.
(14) de Dios, A. C.; Pearson, J. G.; Oldifeld, E. *Science* **1993**, *260*, 1491−1496.
(15) de Dios, A. C.; Oldfield, E. *J. Am. Chem. Soc.* **1994**, *116*, 5307−5314.
(16) Pearson, J. G.; Le, H.; Sanders, L. K.; Godbout, N.; Havlin, R. H.; Oldfield, E. *J. Am. Chem. Soc.* **1997**, *119*, 11941−11950.
(17) Heller, J.; Laws, D. D.; Tomaselli, M.; King, D. S.; Wemmer, D. E.; Pines, A.; Havlin, R. H.; Oldfield, E. *J. Am. Chem. Soc.* **1997**, *119*, 7827−7831.
(18) Mildvan, A. S.; Harris, T. K.; Abeygunawardana, C. *Methods Enzymol.* **1999**, *308*, 219−245.
(19) Frey, P. A.; Whitt, S. A.; Tobin, J. B. *Science* **1994**, *264*, 1927−1930.
(20) Cleland, W. W.; Kreevoy, M. M. *Science* **1994**, *264*, 1887−1890.
(21) Cleland, W. W.; Kreevoy, M. M. *Science* **1995**, *269*, 104.
(22) Frey, P. A. *Science* **1995**, *269*, 104−106.
(23) Cassidy, C. S.; Lin, J.; Frey, P. A. *Biochemistry* **1997**, *36*, 4576−4584.

10.1021/ja0025705 CCC: $19.00
Published on Web 12/05/2000

clarify the situation, we examine here the charge densities in a variety of hydrogen bonds using Bader's theory of atoms in molecules[28] (AIM), and we relate our findings to the observed $^{3h}J_{NC'}$ couplings and ^{1}H chemical shifts. The results provide little evidence for the covalent nature of backbone amide hydrogen bonds in proteins, which appear to be electrostatic or closed-shell in nature.

AIM theory is a powerful quantum mechanical formalism for the analysis of both experimental and theoretical charge densities, $\rho(\mathbf{r})$. Indeed, the past decade has seen its application to virtually all of the naturally occurring amino acids.[29−35] The theory partitions molecular charge distributions into legitimate quantum mechanical subsystems (atoms) based upon features in the gradient vector field of the charge density, $\nabla\rho$. The relative contributions of kinetic and potential energies to individual interactions (bonds) between such atoms can then be determined from the topology of $\rho(\mathbf{r})$, and thus the chemical nature of various atomic interactions can be characterized.[28]

In a rigorous comparison of theoretical and experimental $\rho(\mathbf{r})$ topologies, we recently confirmed that quantum chemical calculations provide excellent descriptions of these properties in both NH···O and OH···O hydrogen bonds.[35] We now apply an AIM energetic analysis to the backbone N−H···O═C hydrogen bonds in the B1 domain of immunoglobulin binding protein G (PGB1), for which $^{3h}J_{NC'}$ couplings have been reported,[1] to clarify the nature of these bonds. We then extend our analysis to include ^{1}H chemical shifts in not only protein G but also several smaller molecules, as well as in enzyme active sites where LBHBs are thought to play a role.[18]

Experimental Section

Charge density calculations were performed by using the Gaussian 94[36] and Gaussian 98[37] programs on a cluster of Silicon Graphics (SGI, Mountain View, CA) Origin-200 computers in this laboratory and on Origin-2000 and Hewlett-Packard (HP, Palo Alto, CA) Exemplar clusters at the National Center for Supercomputing Applications, located in Urbana, IL. For the calculation of charge densities involving the backbone hydrogen bonds of PGB1, we used *N*-formyl-L-alanine amide dimers derived from the protein crystal structure[38] (Research Collaboratory for Structural Bioinformatics Protein Data Bank[39]), truncated with hydrogens at standard bond lengths (Cerius^2, Molecular Simulations Inc., San Diego, CA). The positions of hydrogen and oxygen atoms involved in the N−H···O═C bonds were optimized at the Hartree−Fock (HF) level of theory using the uniform basis set 6-31G(d,p). Charge densities were then calculated by using density functional theory (DFT) with the Becke 3 parameter hybrid exchange functional[40] and the LYP correlation functional,[41] B3LYP. Here, a locally dense basis set scheme was used, which placed 6-311++G(3df,3pd) basis functions on the N−H···O═C moiety and 6-31G(d,p) elsewhere. For hydrogen bond charge densities in other systems, the calculations were performed in the same manner, again using truncated geometries taken from crystal strucures.[42−53] Charge density calculations on fluoromethane dimers were performed using F−C geometries taken from ref 54, and used a uniform 6-311++G(3df,3pd) basis set. The calculations of isolated donor and acceptor (or monomer) charge densities were performed by removing the appropriate bond partner. AIM theory analyses of the resulting charge densities were carried out by using Bader's AIMPAC[55] program package.

Results and Discussion

According to AIM theory each nucleus in a molecule is surrounded by a region called an atomic basin which is bounded by a *zero-flux surface* in $\nabla\rho$ that defines an atomic boundary. When two atoms share some portion of their surfaces, a line of maximum electronic charge density is formed between the nuclei, and at the point where the shared surface intersects this *atomic interaction line* there is a saddle point in $\rho(\mathbf{r})$ called a bond critical point (BCP).[28] In this manner AIM theory identifies

(24) Markley, J. L.; Westler, W. M. *Biochemistry* **1996**, *35*, 11092−11097.
(25) Tobin, J. B.; Whitt, S. A.; Cassidy, C. S.; Frey, P. A. *Biochemistry* **1995**, *34*, 6919−6924.
(26) Garcia-Viloca, M.; Gelabert, R.; Gonzalez-Lafont, A.; Moreno, M.; Lluch, J. M. *J. Phys. Chem. A* **1997**, *101*, 8727−8733.
(27) Schiott, B.; Iversen, B. B.; Madsen, G. K. H.; Bruice, T. C. *J. Am. Chem. Soc.* **1998**, *120*, 12117−12124.
(28) Bader, R. F. W. *Atoms in Molecules−A Quantum Theory*; Clarendon Press: Oxford, 1990.
(29) Flaig, R.; Koritsanszky, T.; Janczak, J.; Krane, H.-G.; Morgenroth, W.; Luger, P. *Angew. Chem., Int. Ed.* **1999**, *38*, 1397−1400.
(30) Gatti, C.; Bianchi, R.; Destro, R.; Merati, F. *J. Mol. Struct.* **1992**, *255*, 409−433.
(31) Destro, R.; Marsh, R.; Bianchi, R. *J. Phys. Chem.* **1988**, *92*, 966−973.
(32) Koritsanszky, T.; Flaig, R.; Zobel, D.; Krane, H.-G.; Morgenroth, W.; Luger, P. *Science* **1998**, *279*, 356−358.
(33) Flaig, R.; Koritsanszky, T.; Zobel, D.; Luger, P. *J. Am. Chem. Soc.* **1998**, *120*, 2227−2238.
(34) Coppens, P.; Abramov, Y.; Carducci, M.; Korjov, B.; Novozhilova, I.; Alhambra, C.; Pressprich, M. *J. Am. Chem. Soc.* **1999**, *121*, 2585−2593.
(35) Arnold, W. D.; Sanders, L. K.; McMahon, M. T.; Volkov, A. V.; Wu, G.; Coppens, P.; Wilson, S. R.; Godbout, N.; Oldfield, E. *J. Am. Chem. Soc.* **2000**, *122*, 4708−4717.
(36) Frisch, M. J.; Trucks, G. W.; Schlegel, H. B.; Gill, P. M. W.; Johnson, B. G.; Robb, M. A.; Cheeseman, J. R.; Keith, T.; Petersson, G. A.; Montgomery, J. A.; Raghavachari, K.; Al-Laham, M. A.; Zakrzewski, V. G.; Ortiz, J. V.; Foresman, J. B.; Cioslowski, J.; Stefanov, B. B.; Nanayakkara, A.; Challacombe, M.; Peng, C. Y.; Ayala, P. Y.; Chen, W.; Wong, M. W.; Andres, J. L.; Replogle, E. S.; Gomperts, R.; Martin, R. L.; Fox, D. J.; Binkley, J. S.; Defrees, D. J.; Baker, J.; Stewart, J. P.; Head-Gordon, M.; Gonzalez, C.; Pople, J. A. *Gaussian 94, Revision C.2*; Gaussian, Inc.: Pittsburgh, PA, 1995.
(37) Frisch, M. J.; Trucks, G. W.; Schlegel, H. B.; Scuseria, G. E.; Robb, M. A.; Cheeseman, J. R.; Zakrzewski, V. G.; Montgomery, J. A., Jr.; Stratmann, R. E.; Burant, J. C.; Dapprich, S.; Millam, J. M.; Daniels, A. D.; Kudin, K. N.; Strain, M. C.; Farkas, O.; Tomasi, J.; Barone, V.; Cossi, M.; Cammi, R.; Mennucci, B.; Pomelli, C.; Adamo, C.; Clifford, S.; Ochterski, J.; Petersson, G. A.; Ayala, P. Y.; Cui, Q.; Morokuma, K.; Malick, D. K.; Rabuck, A. D.; Raghavachari, K.; Foresman, J. B.; Cioslowski, J.; Ortiz, J. V.; Baboul, A. G.; Stefanov, B. B.; Liu, G.; Liashenko, A.; Piskorz, P.; Komaromi, I.; Gomperts, R.; Martin, R. L.; Fox, D. J.; Keith, T.; Al-Laham, M. A.; Peng, C. Y.; Nanayakkara, A.; Gonzalez, C.; Challacombe, M.; Gill, P. M. W.; Johnson, B.; Chen, W.; Wong, M. W.; Andres, J. L.; Gonzalez, C.; Head-Gordon, M.; Replogle, E. S.; Pople, J. A. *Gaussian 98, Revision A.7*; Gaussian, Inc.: Pittsburgh, PA, 1998.
(38) PDB ID: 1PGB. Gallagher, T.; Alexander, P.; Bryan, P.; Gilliland, G. L. *Biochemistry* **1994**, *33*, 4721−4729.
(39) Berman, H. M.; Westbrook, J.; Feng, Z.; Gilliland, G.; Bhat, T. N.; Weissig, H.; Shindyalov, I. N.; Bourne, P. E. *Nucleic Acids Res.* **2000**, *28*, 235−242.
(40) Becke, A. D. *J. Chem. Phys.* **1993**, *98*, 5648−5652.
(41) Lee, C.; Yang, W.; Parr, R. G. *Phys. Rev.* **1988**, *B37*, 785−789.
(42) Ellison, R. D.; Johnson, C. K.; Levy, H. A. *Acta Crystallogr.* **1971**, *B27*, 333−344.
(43) Housty, J.; Hospital, M. *Acta Crystallogr.* **1967**, *22*, 288−295.
(44) Okaya, Y. *Acta Crystallogr.* **1965**, *19*, 879.
(45) PDB ID: 1TPH. Zhang, Z.; Sugio, S.; Komives, E. A.; Liu, K. D.; Knowles, R.; Petsko, G. A.; Ringe, D. *Biochemistry* **1994**, *33*, 2830−2837.
(46) Sequeira, A.; Rajagopal, H.; Ramanadham, H. *Acta Crystallogr.* **1989**, *C45*, 906−908.
(47) Delaplane, R. G.; Ibers, J. A. *Acta Crystallogr.* **1969**, *B25*, 2423−2437.
(48) PDB ID: 6CHA. Tulinsky, A.; Blevins, R. A. *J. Biol. Chem.* **1987**, *262*, 7737−7743.
(49) PDB ID: 1YJA. Kidd, R. D.; Sears, P.; Huang, D. H.; Witte, K.; Wong, C. H.; Farber, G. K. *Protein Sci.* **1999**, *8*, 410−417.
(50) PDB ID: 1QJG. Cho, H.-S.; Ha, N.-; Choi, G.; Kim, H.-J.; Lee, D.; Oh, K. S.; Lee, K. S.; Ki, W.; Choi, K. Y.; Oh, B.-H. *J. Biol. Chem.* **1999**, *274*, 32863−32868.
(51) McGregor, D. R.; Speakman, J. C.; Lehmann, M. S. *J. Chem. Soc., Perkin Trans. 2* **1977**, 1740−1750.
(52) Currie, M.; Speakman, J. C *J. Chem. Soc. A* **1970**, 1923−1926.
(53) Madsen, D.; Flensburg, C.; Larsen, S. *J. Phys. Chem. A.* **1998**, *102*, 2177−2188.
(54) Arnold, W. D.; Mao, J.; Sun, H.; Oldfield, E. *J. Am. Chem. Soc.* **2000,** In press.
(55) Bader, R. F. W. *AIMPAC Program Package*; McMaster University: Hamilton, Ontario, 1998.

a unique line of communication between two chemically interacting nuclei, and provides a unique point at which to probe or characterize the interaction.

The topology of $\rho(\mathbf{r})$ at a BCP is described by the real, symmetric, second-rank Hessian-of-$\rho(\mathbf{r})$ tensor, and the trace of this tensor is related to the bond interaction energy by a *local* expression of the virial theorem:[28]

$$\mathrm{Tr(Hessian)} = \nabla^2\rho(\mathbf{r}) = [2G(\mathbf{r}) + V(\mathbf{r})](4m/\hbar^2) \quad (1)$$

where $\nabla^2\rho(\mathbf{r})$ is the Laplacian of the charge density, $G(\mathbf{r})$ is the electronic kinetic energy density, and $V(\mathbf{r})$ is the electronic potential energy density. These energy densities may be derived from the one-electron density matrix, $\Gamma^{(1)}(\mathbf{r},\mathbf{r}')$:[28]

$$G(\mathbf{r}) = (\hbar^2/2m)\nabla\nabla'\,\Gamma^{(1)}|_{\mathrm{r=r'}}$$

and

$$V(\mathbf{r}) = \mathrm{Tr}[\sigma(\mathbf{r})]$$

where $\sigma(\mathbf{r})$ is the quantum mechanical stress tensor:

$$\sigma(\mathbf{r}) = (\hbar^2/2m)[(\nabla\nabla + \nabla'\nabla') - (\nabla\nabla' + \nabla'\nabla)]\,\Gamma^{(1)}|_{\mathrm{r=r'}}$$

and the primed and unprimed elements refer to ψ^* and ψ, respectively.

Integration of the terms in eq 1 over an atomic basin Ω yields:

$$\int_\Omega \nabla^2\rho(\mathbf{r})\,\mathrm{d}\mathbf{r} = 0;\ \int_\Omega G(\mathbf{r})\,\mathrm{d}\mathbf{r} = T_\Omega;\ \int_\Omega V(\mathbf{r})\,\mathrm{d}\mathbf{r} = \mathrm{V}_\Omega$$

where T_Ω is the total electronic kinetic energy, V_Ω is the total electronic potential energy, and the virial theorem $2T_\Omega = -V_\Omega$ is recovered.[28] Whether they are free or bound within a molecule, these atoms are legitimate, open, quantum mechanical subsystems, subject to all of the theorems of quantum mechanics. Molecules and functional groups are collections of such atomic subsystems, and are themselves bounded by *interatomic* zero-flux surfaces. Since the properties of the subsystems are additive, AIM theory provides a means for the rigorous evaluation of the energetics of not only individual atoms, but also functional groups, molecules, and molecular assemblies.[28] This is a distinct advantage over methods which decompose interaction energy into component terms, such as Morokuma analysis,[56] since such techniques use approximate wave functions which do not satisfy either the virial theorem or the Pauli exclusion principle, and consequently can produce misleading results.[57]

$^{3h}J_{NC'}$ Scalar Coupling. Table 1 lists calculated Laplacians of $\rho(\mathbf{r})$ and energy densities, together with the experimental $^{3h}J_{NC'}$ values measured by Bax and co-workers,[1] for the backbone amide hydrogen bonds in PGB1. Since $G(\mathbf{r})$ must always be positive and $V(\mathbf{r})$ must always be negative in stable, bound, stationary states,[59] the sign of $\nabla^2\rho(\mathbf{r})$ at a BCP is determined by which energy density is in excess over the virial average of 2:1 kinetic-to-potential energy. A negative Laplacian reveals excess potential energy at the BCP, meaning that electronic charge is concentrated into a bond. This is the case in all shared-electron (covalent) interactions. A positive BCP Laplacian reflects an excess of kinetic energy in a bond, and a relative depletion of electronic charge along a bond path. This is the case in all closed-shell (electrostatic) interactions.[28] For every backbone hydrogen bond examined (Table 1) $\nabla^2\rho(\mathbf{r})$ is positive and characteristic of a closed-shell atomic interaction. Figure 1 shows the correlation between the magnitude of each term in the local virial expression (eq 1) and the magnitude of the scalar coupling, $|^{3h}J_{NC'}|$, for the β sheet hydrogen bonds in PGB1. Although each term increases exponentially as $|^{3h}J_{NC'}|$ increases, the kinetic term is a slightly stronger exponential in this region, and outpaces the increase in the potential term. It

Table 1. Bond Critical Point Laplacians and Energy Densities, $^{3h}J_{NC'}$-Couplings, and $^1H^N$ Chemical Shifts for Helix and Sheet Backbone Hydrogen Bonds in PGB1

donor/2° structure	$\nabla^2\rho(\mathbf{r})^a$ ($e a_o^{-5}$)	$G(\mathbf{r})^b$ ($e^2 a_o^{-4}$)	$V(\mathbf{r})^c$ ($e^2 a_o^{-4}$)	$H(\mathbf{r})^d$ ($e^2 a_o^{-4}$)	$^{3h}J_{NC'}{}^e$ (Hz)	δ^1H^f (ppm)
3/β_s	0.0820	0.0179	−0.0152	0.0027	−0.51	9.17
4/β_s	0.0625	0.0131	−0.0106	0.0025	−0.42	9.05
5/β_s	0.0973	0.0219	−0.0196	0.0023	−0.70	8.57
7/β_s	0.0978	0.0226	−0.0207	0.0019	−0.68	8.67
8/β_s	0.0923	0.0204	−0.0177	0.0027	−0.70	8.87
9/β_s	0.0665	0.0138	−0.0110	0.0028	−0.33	7.89
14/β_s	0.0456	0.0095	−0.0077	0.0018	−0.24	8.39
16/β_s	0.0584	0.0123	−0.0099	0.0024	−0.38	8.71
18/β_s	0.0681	0.0143	−0.0116	0.0027	−0.41	9.01
20/β_s	0.0858	0.0185	−0.0155	0.0030	−0.51	9.24
42/β_s	0.0646	0.0138	−0.0115	0.0023	−0.43	8.15
44/β_s	0.0737	0.0160	−0.0135	0.0025	−0.53	9.24
46/β_s	0.0614	0.0129	−0.0104	0.0025	−0.36	7.58
51/β_s	0.0498	0.0103	−0.0082	0.0021	−0.22	7.34
52/β_s	0.1094	0.0256	−0.0238	0.0018	−0.70	10.34
53/β_s	0.0923	0.0206	−0.0181	0.0025	−0.61	9.08
54/β_s	0.0604	0.0125	−0.0099	0.0026	−0.39	8.13
55/β_s	0.0841	0.0188	−0.0166	0.0022	−0.51	8.31
56/β_s	0.0531	0.0109	−0.0085	0.0024	−0.33	7.77
26/α_h	0.0461	0.0095	−0.0076	0.0019	−0.18	7.08
27/α_h	0.0547	0.0114	−0.0092	0.0022	−0.54	8.30
28/α_h	0.0198	0.0040	−0.0030	0.0010	−0.13	6.92
29/ α_h	0.0453	0.0093	−0.0073	0.0020	−0.21	7.25
30/α_h	0.0801	0.0175	−0.0149	0.0026	−0.64	8.47
31/α_h	0.0767	0.0167	−0.0141	0.0026	−0.72	9.05
32/α_h	0.0477	0.0098	−0.0077	0.0021	−0.19	7.37
33/α_h	0.0744	0.0160	−0.0135	0.0025	−0.27	8.21
34/α_h	0.0854	0.0188	−0.0163	0.0025	−0.49	9.17
35/α_h	0.0877	0.0195	−0.0171	0.0024	−0.31	8.23
36/α_h	0.0950	0.0217	−0.0196	0.0021	−0.60	8.90

[a] Laplacian of the charge density. [b] Kinetic energy density. [c] Potential energy density. [d] Total energy density. [e] Trans hydrogen bond scalar coupling, ref 1. [f] $^1H^N$ chemical shift at pH 5.4, ref 58.

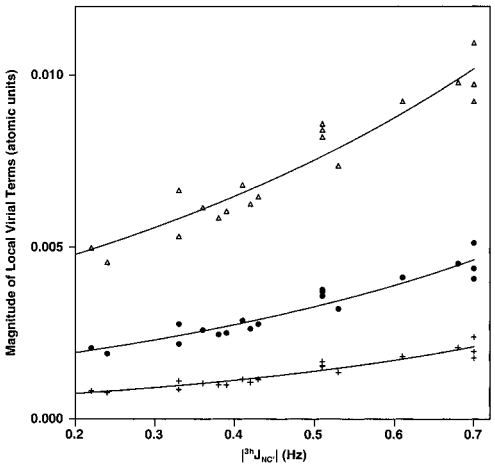

Figure 1. The magnitude of terms in the local virial expression versus the magnitude of $^{3h}J_{NC'}$: $\Delta = \nabla^2\rho(\mathbf{r})$, $\nabla^2\rho(\mathbf{r}) = 0.035\ \exp[1.5|J|]$, $R^2 = 0.91$; $\bullet = 2G(\mathbf{r})$, $2G(\mathbf{r}) = 0.014\ \exp[1.8|J|]$, $R^2 = 0.91$; $+ = V(\mathbf{r})$, $|V(\mathbf{r})| = 0.0049\ \exp[2.1|J|]$, $R^2 = 0.90$.

(56) Morokuma, K. *J. Chem. Phys.* **1971**, *55*, 1236−1244.
(57) Janda, K. C.; Steed, J. M.; Novic, S. E.; Klemperer, W. *J. Chem. Phys.* **1977**, *67*, 5162−5172.
(58) Orban, J.; Alexander, P.; Bryan, P.; Khare, D. *Biochemistry* **1995**, *34*, 15291−15300.
(59) Bader, R. W. F. *J. Phys. Chem. A* **1998**, *102*, 7314−7323.

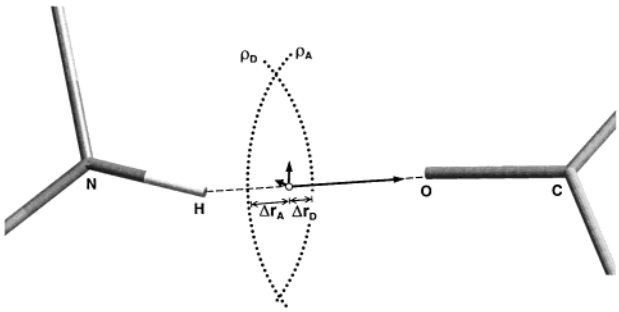

Figure 2. A schematic representation of a typical N−H···O═C hydrogen bond, depicting the atomic interaction line (dashed line), the Hessian tensor (solid arrows), the BCP (○), and the nonbonding van der Waals shells of the isolated hydrogen bond donor and acceptor molecules (ρ_D and ρ_A, dotted curves). The distance Δr_D is the penetration of the BCP into ρ_D, and the distance Δr_A is the penetration of the BCP into ρ_A.

can therefore immediately be seen that not only are these hydrogen bonds closed-shell interactions ($\nabla^2\rho(\mathbf{r}) > 0$), but that the net amount of excess kinetic energy density is greatest for the largest couplings. This could not be the case if such couplings were dependent upon, or indicative of, covalent character in the bonds.

While we show only the 19 sheet residues in PGB1, the correlations shown in Figure 1 still exist if we include all the residues given in Table 1. However, among the eleven helical residues there are four outliers (E27, K31, Y33, and N35), and these decrease the coeffecients of determination, R^2, from 89−90% (Figure 1) to 66−69%. It seems noteworthy that of the four outliers, three belong to the same ($i + 4$) hydrogen bond network, and may reflect small crystal−solution structural differences, which are nevertheless significant on the scale of $^{3h}J_{NC'}$. Rather than arbitrarily rejecting these points, Figure 1 focuses on the β sheet residues as a class, and none of the conclusions drawn regarding $^{3h}J_{NC'}$ and the nature of the backbone hydrogen bonds would be changed by considering all of the residues in Table 1.

Although the kinetic energy term provides the dominant virial contribution, resulting in a net closed-shell, electrostatic interaction, we must now consider whether these interactions represent a closed-shell limit by evaluating the total energy density, $H(\mathbf{r})$, at the BCP:[60]

$$H(\mathbf{r}) = G(\mathbf{r}) + V(\mathbf{r}) \qquad (2)$$

The electronic potential energy of a stable system in electrostatic equilibrium is always negative, or stabilizing.[59] A negative total energy density at the BCP reflects a dominance of potential energy density, and is the consequence of accumulated stablilizing electronic charge. Thus the condition in which $|V(\mathbf{r})| < 2G(\mathbf{r})$ (eq 1), but $|V(\mathbf{r})| > G(\mathbf{r})$ (eq 2), has been termed *partially* covalent.[61] Bonds with *any* degree of covalent character (any amount of potential energy stabilization resulting from the accumulation of charge in the internuclear region) must have a BCP $H(\mathbf{r})$ which is less than zero. Our results for the PGB1 backbone hydrogen bonds provide no evidence of partial covalent character (Table 1), $H(\mathbf{r}) > 0$ in all cases. The backbone hydrogen bonds appear to represent purely closed-shell, electrostatic interactions.

If $^{3h}J_{NC'}$ does not arise from a partial covalent interaction, then what permits the intermolecular communication between nuclear spins? Figure 2 shows a schematic representation of a typical N−H···O═C hydrogen bond. An AIM atomic interaction line (dashed line) connects the hydrogen and oxygen nuclei. The hydrogen bond Hessian tensor, seen here in its principal axis system (solid arrows), lies on this line at the BCP (○). Also depicted are the nonbonding van der Waals shells of the isolated hydrogen bond donor and acceptor molecules ($\rho(\mathbf{r}) = 0.001$ e/a_o^3, dotted curves). The distance Δr_D is the penetration of the BCP into the nonbonding charge density shell of the donor, ρ_D. Likewise, Δr_A is the penetration of the BCP into the nonbonding shell of the acceptor, ρ_A.[28] The mutual penetration, $\sum\Delta r$, of the donor and acceptor van der Waals shells is the sum $\Delta r_A + \Delta r_D$, and each of these distances is listed in Table 2 for the sheet residues of PGB1. Figure 3 shows that the magnitude of $^{3h}J_{NC'}$ is clearly related to the mutual penetration of nonbonding van der Waals shells. However, as Carroll and Bader have shown for a wide array of base−HF complexes,[62] there is no concentration of charge in the bonding region upon complex (or hydrogen bond) formation. Thus, as shown in Figure 4, the electron density in the hydrogen bond is simply the sum of isolated donor and acceptor densities: the greater the van der Waals penetration, the greater the resulting summed electron density and the greater the experimentally observed *J*-coupling.

This description of $^{3h}J_{NC'}$ also provides a simple physical explanation for the existence of scalar couplings between nuclei which cannot possibly be covalently bonded to one another. For example, Kimber et al.[13] observed a field-independent ^{19}F−^{19}F coupling of 17(±2) Hz in a dihydrofolate reductase (DHFR)−NADPH−methotrexate complex which had been prepared biosynthetically with 6-fluorotryptophan residues. With no crystal structure of DHFR available, these researchers postulated that two of the four 6-fluorotryptophan residues must be situated such that their ^{19}F nuclei are roughly 3 Å apart, based upon much earlier empirical observations of "through space" ^{19}F−^{19}F *J*-couplings in small organic molecules.[13]

Table 2. Penetration of Hydrogen Bond Donor and Acceptor Nonbonding van der Waals Densities in PGB1

donor − acceptor	Δr_D[a] (Å)	Δr_A[b] (Å)	$\sum\Delta r$[c] (Å)	$(\rho_d^\circ + \rho_a^\circ)$[d] ($ea_o^{-3}$)	$\rho(\mathbf{r})$[e] (ea_o^{-3})
Y3−T18	0.4973	0.5087	1.0060	0.0199	0.0198
K4−K50	0.4522	0.4736	0.9258	0.0158	0.0155
L5−T16	0.5400	0.5512	1.0912	0.0240	0.0239
L7−G14	0.5422	0.5676	1.1098	0.0251	0.0248
N8−V54	0.5228	0.5259	1.0487	0.0222	0.0220
G9−L12	0.4601	0.4701	0.9302	0.0162	0.0158
G14−L7	0.3964	0.4624	0.8588	0.0125	0.0123
T16−L5	0.4387	0.4700	0.9087	0.0151	0.0150
T18−Y3	0.4652	0.4848	0.9500	0.0168	0.0165
A20−M1	0.4932	0.5074	1.0006	0.0199	0.0200
E42−T55	0.4610	0.5000	0.9610	0.0169	0.0168
T44−T53	0.4853	0.5306	1.0159	0.0190	0.0189
D46−T51	0.4441	0.4599	0.9040	0.0153	0.0152
T51−D46	0.4076	0.4250	0.8326	0.0129	0.0128
F52−K4	0.5737	0.5977	1.1714	0.0278	0.0276
T53−T44	0.5272	0.5631	1.0903	0.0232	0.0231
V54−I6	0.4383	0.4418	0.8801	0.0147	0.0144
T55−E42	0.5160	0.5478	1.0638	0.0218	0.0218
E56−N8	0.4493	0.4490	0.8983	0.0142	0.0131

[a] Penetration of the BCP into the nonbonding van der Waals shell of the hydrogen bond donor. [b] Penetration of the BCP into the nonbonding van der Waals shell of the hydrogen bond acceptor. [c] Mutual penetration of nonbonding van der Waals shells. [d] ρ_d° is the charge density in the isolated hydrogen bond donor at the point where the BCP exists in the hydrogen-bonded complex, and ρ_a° is the charge density in the isolated hydrogen bond acceptor at the same point. [e] Charge density at the hydrogen bond BCP.

(60) Cremer, D.; Kraca, E. *Croat. Chem. Acta* **1984**, *57*, 1259−1281.
(61) Jenkins, S.; Morrison, I. *Chem. Phys. Lett.* **2000**, *317*, 97−102.
(62) Carroll, M. T.; Bader, R. F. W. *Mol. Phys.* **1988**, *65*, 695−722.

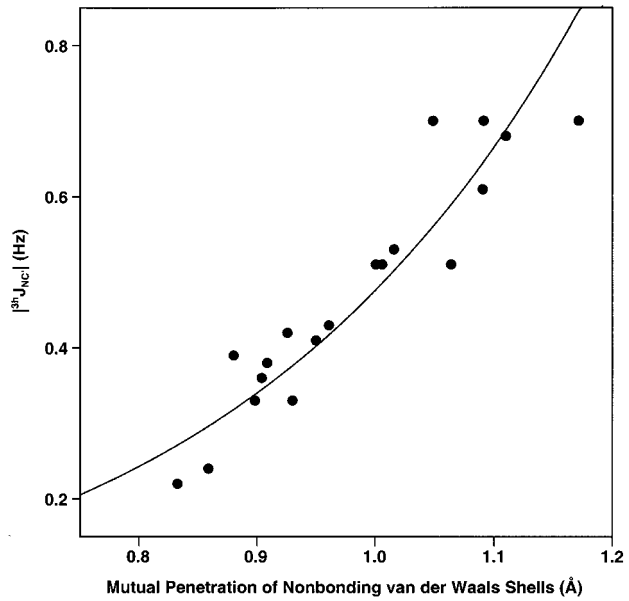

Figure 3. The exponential dependence of the magnitude of $^{3h}J_{NC'}$ couplings upon the mutual penetration of nonbonding van der Waals shells, $\sum\Delta r$. $|^{3h}J_{NC'}| = 0.017 \exp[3.36\sum\Delta r]$, $R^2 = 0.86$.

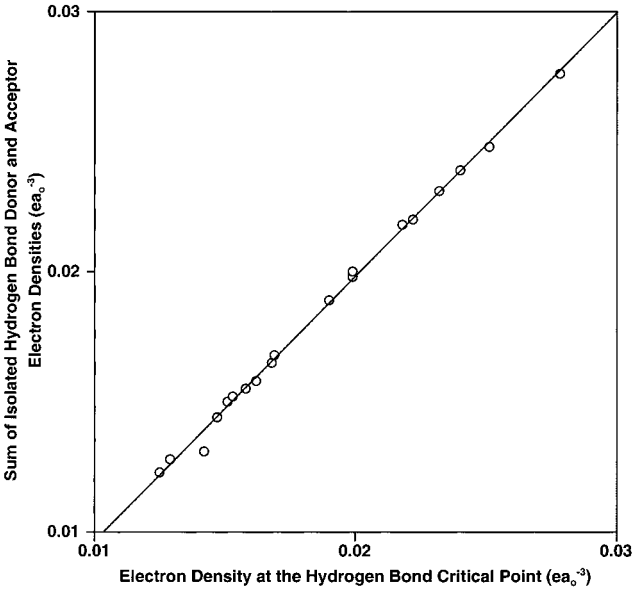

Figure 4. The sum of isolated hydrogen bond donor and acceptor charge densities versus the charge density at the hydrogen bond BCP. The isolated densities are taken at the point where the BCP exists in the hydrogen bonded complex. Slope = 1.02, $R^2 = 0.997$.

Subsequently, it was found that the folded protein brings the 6-positions of Trp5 and Trp133 into extremely close proximity,[63] and in a separate investigation, we have found that sum-over-states density functional theory (SOS-DFT) predicts a $^{19}F-^{19}F$ coupling of 32.9 Hz between two fluoromethane molecules at 2.98 Å separation.[54] An AIM atomic interaction line indeed exists between the two ^{19}F nuclei, and the nonbonding van der Waals shells of the monomers penetrate one another by 0.47 Å along this line (Table 3). We have also recently shown that long-range ($^{>3}J_{FF}$), intramolecular $^{19}F-^{19}F$ through-space *J*-couplings in a wide range of systems are well described by SOS-DFT calculations, and that small, nonbonded dimer models such as $(CH_3F)_2$ give very similar results to covalently bonded models.[54]

(63) PDB ID: 3DFR. Bolin, J. T.; Filman, D. J.; Matthews, D. A.; Hamlin, R. C.; Kraut, J. *J. Biol. Chem.* **1982**, *237*, 13650−13662.

Table 3. Penetration of Monomer Nonbonding van der Waals Densities in Difluoromethane Dimers

molecule[a]	Δr_{F1}[b] (Å)	Δr_{F2}[c] (Å)	$\sum\Delta r$[d] (Å)	J_{FF}[e] (Hz)
6c	0.4837	0.4839	0.9676	85.2
6d	0.4369	0.4364	0.8733	59
6e	0.4470	0.4459	0.8929	66.1
6f	0.4465	0.4463	0.8928	65.6
7b	0.3411	0.3405	0.6816	36.7
7d	0.3613	0.3611	0.7224	28.8
9	0.5283	0.5284	1.0567	∼170
DHFR	0.2350	0.2337	0.4686	17

[a] Numbering scheme is that of ref 54. [b] Penetration of the BCP into the nonbonding van der Waals shell of fluoromethane monomer 1. [c] Penetration of the BCP into the nonbonding van der Waals shell of fluoromethane monomer 2. [d] Mutual penetration of nonbonding van der Waals shells. [e] Experimental through-space $^{19}F-^{19}F$ scalar couplings: ref 54 and cited references therein.

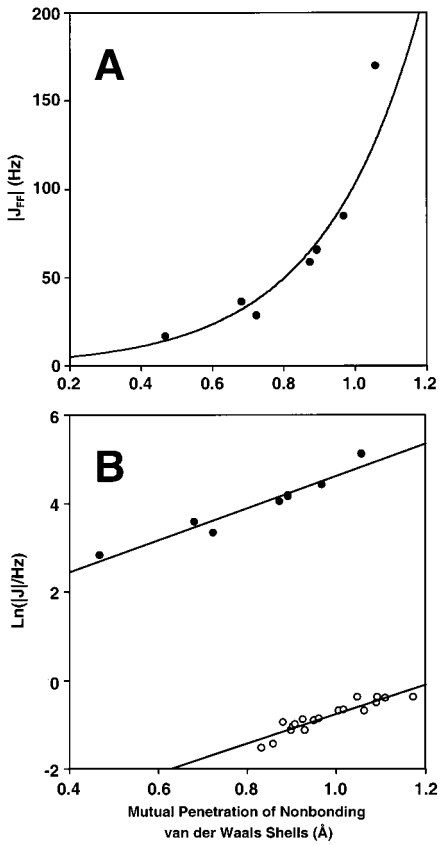

Figure 5. (A) The exponential dependence of the magnitude of through-space $^{19}F-^{19}F$ *J*-couplings upon the mutual penetration of nonbonding van der Waals shells, $\sum\Delta r$. $|J_{FF}| = 2.6 \exp[3.67\sum\Delta r]$, $R^2 = 0.94$. (B) Ln(|*J*|) versus $\sum\Delta r$. ● = J_{FF}, ○ = $^{3h}J_{NC'}$.

We therefore investigated the extent of the van der Waals penetration in several more fluoromethane dimers, whose F−C geometries were extracted from larger, organic molecules possessing such long-range J_{FF}-couplings[54] (Table 3). It has been well-established that the magnitudes of both J_{FF} and $^{3h}J_{NC'}$ increase exponentially with decreasing internuclear separation,[1,64] and Figure 5 shows that these magnitudes are related to the mutual penetration of nonbonding van der Waals shells in the same manner: both are of the exponential form $|J| = A \exp[B\sum\Delta r]$, where *B* is 3.36 for $^{3h}J_{NC'}$ and 3.67 for J_{FF}. The

(64) Mallory, F. B.; Mallory, C. W.; Butler, K. E.; Lewis, M. B.; Xia, A. Q.; Luzik, E. D., Jr.; Fredenburgh, L. E.; Ramanjulu, M. M.; Van, Q. N.; Francl, M. M.; Freed, D. A.; Wray, C. C.; Hann, C.; Nerz-Stormes, M.; Carroll, P. J.; Chirlian, L. E. *J. Am. Chem. Soc.* **2000**, *122*, 3560−3561.

Table 4. Hydrogen Bond Local Energy Densities and Chemical Shifts in Model Systems and Proteins

structure[a]	δ^1H[b] (ppm)	$V(\mathbf{r})$ ($e^2a_o^{-4}$)	$G(\mathbf{r})$ ($e^2a_o^{-4}$)	$H(\mathbf{r})$ ($e^2a_o^{-4}$)	$\nabla^2\rho(\mathbf{r})$ (ea_o^{-5})
glycolic acid[42] (COH− O)	7.3[67]	−0.029	0.028	−0.001	0.111
glycolic acid[42] (COH− O)	7.7[67]	−0.024	0.026	0.001	0.108
glycolic acid[42] (CO_2H−O)	12.4[67]	−0.044	0.036	−0.008	0.115
azeleic acid[43]	12.9[67]	−0.047	0.036	−0.011	0.102
KH phthalate[44]	14.0[67]	−0.038	0.032	−0.006	0.105
TIM-PGH[c] (E165−PGH[45])	14.9[68]	−0.067	0.049	−0.018	0.124
aspartic acid[46]	15.4[67]	−0.052	0.039	−0.013	0.103
oxalic acid[47]	16.9[67]	−0.057	0.037	−0.020	0.068
chymotrypsin-BoroPhe[d] (H57−D102[48])	16.9[68]	−0.066	0.050	−0.016	0.133
substilisin-BoroPhe[d] (H64−D32[49])	17.4[68]	−0.079	0.049	−0.030	0.072
KIS-equilenin[e] (D99-Y14[50])	17.5[68]	−0.045	0.035	−0.010	0.098
KH dicrotonate[51]	18.2[67]	−0.089	0.056	−0.033	0.090
KH malonate[52]	20.5[67]	−0.113	0.064	−0.049	0.061
KH maleate[53]	21[67]	−0.272	0.084	−0.188	−0.416

[a] Crystal structure reference. [b] X(^{1}H)−A chemical shift. [c] Triosephosphate isomerase complex with phosphoglycolohydroxamic acid. [d] Methoxysuccinyl-A-A-P-2-amino-3-phenylethylboronic acid. [e] Ketosteroid isomerase complex with dihydroequilenin.

fact that ln[|J|] versus $\sum\Delta r$ has a very similar slope for both types of couplings strongly suggests that the through-space J_{FF} coupling and the hydrogen bond $^{3h}J_{NC'}$ coupling are subject to the same inductive mechanism, and require neither an attractive electrostatic bond nor a covalent bond, only that two atomic surfaces contact one another in the intervening space between coupled nuclei.

Chemical Shifts in Hydrogen Bonds. Using the ^{1}H chemical shift as a probe, we now apply the same AIM energy analysis to a wider array of hydrogen bonds, including short, strong hydrogen bonds (SSHB) in enzymes and an intramolecular LBHB. For the enzymatic systems we use the less controversial term SSHB, since this avoids the question as to whether LBHBs actually form in solvated active sites. In a comprehensive survey of 83 experimental $\rho(\mathbf{r})$ topologies, Espinosa et al. have demonstrated that the BCP Laplacians and energy densities of essentially all hydrogen bonds exhibit the same behavior, regardless of type, and can be considered together.[65−67] In Table 4 we list X(^{1}H)···A chemical shifts together with the local (kinetic, potential, and total) energy densities at BCPs for hydrogen bonds in several carboxylic acids, as well as for the SSHBs in several enzymes complexed with reaction intermediate/transition-state analogues. These and the corresponding PGB1 data (Table 1) are plotted as a function of the ^{1}H chemical shift (δ, in ppm from tetramethylsilane) in Figure 6, where it can be seen that the local energy densities exhibit an exponential dependence upon $\delta(^1$H). A change in the proton chemical shift corresponds to a change in the character of the hydrogen bond: between 12 and 14 ppm partial covalent character begins to develop as the ^{1}H nucleus becomes less shielded. While the dominant virial interaction is still closed-shell in nature, covalence increases sharply as $H(\mathbf{r})$ becomes exponentially more negative (eq 2) to ∼21 ppm, which represents a maximum

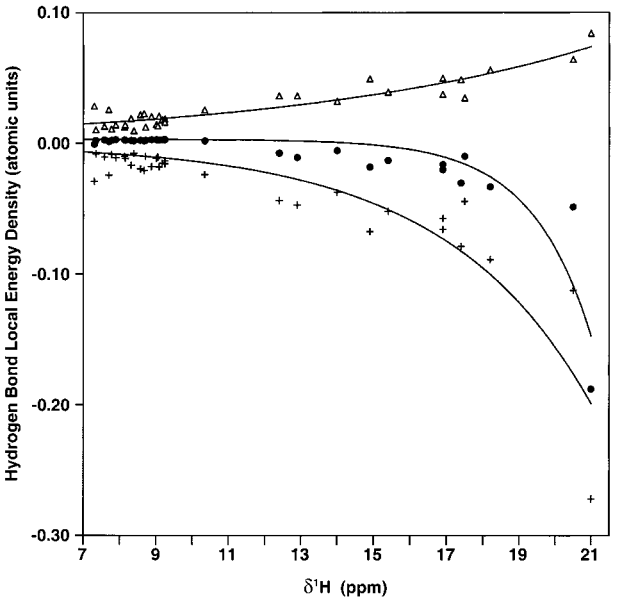

Figure 6. The dependence of the hydrogen bond local energy densities upon the proton chemical shift: $\Delta = G(\mathbf{r})$, $G(\mathbf{r}) = 0.0066\exp[0.12\delta]$, $R^2 = 0.87$; ● = $H(\mathbf{r})$, $H(\mathbf{r}) = (-6.1\times10^{-7})\exp[0.59\delta] - 0.003$, $R^2 = 0.83$; + = $V(\mathbf{r})$, $V(\mathbf{r}) = -0.0012\exp[0.24\delta]$, $R^2 = 0.82$.

value.[68,69] The points at 20.5 and 21 ppm correspond to hydrogen malonate and hydrogen maleate, respectively (Table 4), which have each been shown to contain an intramolecular LBHB.[70] A LBHB is formed when the energy barrier for the transfer of hydrogen from the donor to acceptor is close to the zero-point vibrational energy of the hydrogen. The zero-point energy for deuterium, being lower than that of hydrogen, means that a deuterium atom does not experience the same low energy barrier for transfer, and remains localized at the hydrogen bond donor. However, high-resolution X-ray and neutron diffraction studies of deuterated hydrogen maleate have found that the O−^{2}H−O moiety is symmetric; the deuterium atom is equidistant from either oxygen in the intramolecular hydrogen bond.[53] This bond, therefore, represents a limiting case of the LBHB, in which the hydrogen atom experiences a single-well potential. Furthermore, AIM analysis of the experimental maleate $\rho(\mathbf{r})$ has shown that the bonds in O−H−O are shared-electron, covalent bonds ($\nabla^2\rho(\mathbf{r}) < 0$).[53] Indeed, the exponential fits of the data in Table 4 and Figure 6 nicely confirm that at after approximately 20 ppm the potential energy density, $V(\mathbf{r})$, finally begins to dominate the kinetic energy density, $G(\mathbf{r})$, in terms of the local virial expression (eq 1), and that the hydrogen bond becomes a genuine shared-electron or covalent interaction.

Among the proponents of LBHB enzyme catalysis, hydrogen bonds are believed to strengthen during the formation of a reaction intermediate or transition state, with the donor and acceptor atoms being closer together than they are in the substrate and situated such that the hydrogen atom is roughly equidistant between them, being covalently bonded to both.[20] A downfield ^{1}H NMR chemical shift of approximately 15−20 ppm has been one of the primary criteria used to identify these potential catalytic LBHBs.[18] The results in Table 4 indicate that, unlike backbone hydrogen bonds, there is indeed significant partial covalent bonding character between the closer hydrogen atom and the acceptor oxygen atom in this chemical shift range,

(65) Espinosa, E.; Souhassou, M.; Lachekar, H.; Lecomte, C. *Acta Crystallogr.* **1999**, *B55*, 563−572.
(66) Espinosa, E.; Lecomte, C.; Molins, E. *Chem. Phys. Lett.* **1999**, *300*, 745−748.
(67) Espinosa, E.; Molins, E.; Lecomte, C. *Chem. Phys. Lett.* **1998**, *285*, 170−173.
(68) Harris, R. K.; Jackson, P.; Merwin, L. H.; Say, B. J. *J. Chem. Soc., Faraday Trans. 1* **1988**, *84*, 3649−3672.
(69) Harris, T. K.; Mildvan, A. S. *Proteins* **1999**, *35*, 275−282.
(70) Garcia-Viloca, M.; Gelabert, R.; Gonzalez-Lafont, A.; Moreno, M.; Lluch, J. M. *J. Phys. Chem. A* **1997**, *101*, 8727−8733.

and that the furthur downfield the ^{1}H resonates, the greater the covalent character becomes. Since it has already been demonstrated that $\delta(^1\text{H})$ increases exponentially as the hydrogen bond distance OH···O decreases,[71] and since enzymatic SSHBs are found at the steep ends of the energy density exponentials (Figure 6), small perturbations in donor−acceptor distances have very large energetic consequences. In this sense, it is a relatively short trip from the partially covalent SSHBs at 15−20 ppm to the shared-electron, single-well LBHB at 21 ppm.

Conclusions

The results we have presented above are of interest for several reasons. First, we have related AIM theory local energy densities found in hydrogen bonds to NMR observables. In so doing, we have been able to correlate the chemical nature of these bonds with the magnitudes of the trans hydrogen bond scalar couplings and the proton chemical shifts. Second, our results indicate that the $^{3h}J_{NC'}$ couplings observed in proteins are mediated by closed-shell, noncovalent NH···OC interactions. The inductive mechanism which allows the nitrogen and carbon nuclei to couple is provided by a mutual penetration of isolated donor and acceptor nonbonding van der Waals charge densities. Third, our results show that this same mechanism explains the through-space scalar couplings observed between fluorine nuclei in organic molecules and in a protein. Fourth, our results show that the magnitudes of both $^{3h}J_{NC'}$ and J_{FF} depend on a very similar exponential function of van der Waals penetration. Fifth, we have observed that hydrogen bond ^{1}H chemical shifts describe a wide range of chemical interactions, from the closed-shell limit in protein backbone hydrogen bonds, to the partially covalent in enzymatic SSHBs, to the genuine shared-electron in LBHBs. As the proton resonates at lower and lower field, there is a smooth, exponential increase in the degree of covalence in the hydrogen bond, until at about 20−21 ppm the bond becomes a genuine shared-electron (covalent) interaction. Sixth, our results indicate that the SSHBs observed in enzyme active sites, having ^{1}H NMR chemical shifts in the 15−20 ppm range, have significant covalent character, and seem poised to become full-fledged shared-electron interactions in response to small fluctuations in protein structure. This supports the idea that the SSHB donor and acceptor distances may close during formation of a transition state LBHB, creating a state in which the hydrogen has shared-electron interactions with both donor and the acceptor atoms.

Acknowledgment. This work was supported by the United States Public Health Service (NIH grant GM-50694), and was carried out in part by use of the SGI/Cray Origin 2000 and HP Exemplar clusters at the National Center for Supercomputing Applications, Urbana, IL (funded in part by the National Computational Science Alliance, grant MCA-98N039).

JA0025705

(71) McDermott, A.; Ridenour, C. F. *Encyclopedia of NMR*; Wiley: Sussex, UK, 1996; pp 3820−3825.